Mach number measurement in W49A?

Mention works by Shetty, Glover, Clark.

Here is some confusion about (mix of) IMF papers, which are Padoan & Nordlund 2002, 2007; Hennbelle & Chabrier 2008, 2009; Hopkins 2012, 2013 and on the other hand the SFR, which are Krumholz & McKee 2005, Padoan & Nordlund 2011, Hennebelle & Chabrier 2011, Federrath & Klessen 2012.

Molecular Density Measurements with H_2CO: Turbulence is Compressively Driven

ABSTRACT

Molecular clouds are supersonically turbulent. This turbulence may govern the form of the initial mass function and the star formation rate of the gas. It is therefore essential to understand the properties of turbulence, in particular the probability distribution of

density measurements of a non-star-forming cloud along
A. This method is complementary to measurements of tur-
y distribution and should be applicable to any molecular
show that turbulence in this cloud must be compressively
-total ratio $b = \mathcal{M}_C/\mathcal{M} > 0.6$.

Maybe we should mention here not only the IMF, but also the SFR (Krumholz & McKee 2005, Padoan & Nordlund 2011, Hennebelle & Chabrier 2011, Federrath & Klessen 2012). BTW: Does Krumholz et al 2005 really predict much about the IMF? I thought those are single cores and only produce essentially one massive star and a few MUCH LOWER mass stars around it. Hardly an IMF and hardly a theroy for it, isn't it?

Use ordering by publication year (date). Same applies to all the following cases with citation lists further down in the paper.

1. Introduction

Nearly all gas in the interstellar medium is supersonically turbulent. The properties of this turblence are essential for determining how star formation progresses. There are now predictive theories of star formation that include formulations of the Initial Mass Function (Hopkins 2012; Chabrier & Hennebelle 2010; Hennebelle & Chabrier 2011, 2013; Padoan et al. 2012; Padoan & Nordlund 2011; Padoan et al. 2007; Krumholz et al. 2005). The distribution of stellar masses
roperties of the turbulence. It is therefore essential to measure the
he molecular clouds that produce these stars.

Add Price et al. 2011, but Kritsuk et al. 2011 is not really on different driving, but on the PDF in self-graviating turbulence.

d simulations to characterize the density distribution from different driving modes of turbulence (Federrath & Klessen 2013; Federrath et al. 2011, 2010, 2009, 2008; Kritsuk et al. 2011). These works determined that there is a relation between the mode of turbulent driving and the width of the turbulent distribution, with $\sigma_{\ln\rho} = \ln\left(1 + b^2\mathcal{M}^2\frac{\beta}{\beta+1}\right)$, where $\beta = 2(\mathcal{M}_A/\mathcal{M})^2 = 2(c_s/v_A)^2$. This equation can also be expressed in terms of the compressive mach number $\mathcal{M}_c = b\mathcal{M}$, with $b \approx 1/3$ corresponding to solenoidal forcing and $b = 1$ corresponding to
ssive forcing (Federrath et al. 2010; Konstandin et al. 2012; Molina et al. 2012).

Must be sigma_s SQUARED.

(Padoan & Nordlund 2011, Moina et al. 2012)

All of the turbulence-based theories of star formation explicitly assume a lognormal form for the density probability distribution $P_V \ln\rho$ of the gas. However, recent simulations (Federrath & Klessen 2013) and theoretical work (Hopkins 2013) have shown that the assumption of a lognormal distribution is often very poor[1], deviating by orders of magnitude at the extreme of the density

[1] lognormal mass-weighted and volume-weighted density distribution is also not

P_V(s). I think it would be good maybe to introduce the log-density contrast s=ln(rho/rho_0). I don't really like writing ln(rho), because when taking the logarithm of a quantity it must always be divided first by a quantity with the same units, in this case the units of density.

Actually, we find that the effect of the power-law tail on the SFR is not very strong, because the tail developes along with the onset of star formation. So, the SFR is rather determined by the state when the power-law tail caused by collapse has not yet developed, and then the tail just developes as a result of star formation (collapse), but does not have a strong influence on star formation itself.

However, the point you are trying to make about non-lognormal features is fine, because also in the non-self-gravitating stage (before the high-density power-law developes), the PDFs are NOT perfectly log-normal, which might introduce some corrections to the SFR. So, in that sense, it is useful that you consider the Hopkins intermittency PDFs (but you have to seprate this from the high-density power-law tail, which is not caused by intermittency, but by gravitational collapse).

distributions. Since these theories all involve an integral over the density probability distribution funcion (PDF), skew in the lognormal distribution can drastically affect the overall star formation rate and predicted initial mass function.

While simulations are powerful probes of wide ranges of parameter space, no simulation is capable of including all of the physical processes and spatial scales relevant to turbulence. Observations are required to provide additional constraints on properties of interstellar turbulence and guide simulators towards the most useful conditions and processes to include. Kainulainen et al. (2013) and Kainulainen & Tan (2012) provide some of the first observational constraints on the mode of turbulent driving, finding $b \approx 0.4$, i.e. that there is a mix of solenoidal and compressive modes.

Mention also Brunt 2010, who finds b~0.5.

Formaldehyde, H_2CO, is a unique probe of density in molecular clouds. Like CO, it is ubiquitous, with a nearly constant abundance wherever CO is found (Tang et al. 2013; Mangum & Wootten 1993). The lowest rotational transitions of o-H_2CO at 2 and 6 cm can be observed in absorption against the cosmic microwave background or any bright continuum source (Ginsburg et al. 2011; Darling & Zeiger 2012). The ratio of these lines is strongly sensitive to the local density of H_2, but it is relatively insensitive to the local gas temperature (Wiesenfeld & Faure 2013; Troscompt et al. 2009). Unlike critical density tracers, the H_2CO line ratio has a direct dependence on the density that is independent of the column density.

However, the particular property of the H_2CO densitometer we explore here is its ability to trace the *mass-weighted* density of the gas. Typical density measurements from ^{13}CO or dust measure the total mass and assume a line-of-sight geometry, measuring a *volume-weighted* density, i.e. $\rho_V = M_{tot}/V_{tot}$. In contrast, the H_2CO densitometer is sensitive to the density that corresponds to the most mass, i.e. $\rho_M = \int M \rho dM / M_{tot}$. The volume- and mass- weighted densities will vary with different drivers of turbulence, so in clouds dominated by turbulence, if we have measurements of both, we can infer the driver.

Sounds strange. Maybe rephrase.

In Ginsburg et al. (2011), we noted that the H_2CO densitometer revealed volume densities much higher than expected given the cloud-average densities from ^{13}CO observations. The densities were higher even than typical turbulence will allow. However, this argument was made on the basis of a statistical argument; here we attempt to demonstrate that the clumps in GMCs are of very high density in individual clouds.

"statistical average over many clouds"? Is that what you mean?

We should be more precise here. Can you elaborate a bit on what you do when you compare rho_V with rho_M to get the mode mixture of the driver? Also, note that we cannot really get the driver (e.g., supernova, jets, callapse, HII region, ...), but only the mode mixture that this driver corresponds to (or excites), i.e., we can possibly get the b parameter, but not the phyiscal source of the turbulence (the actual driver).

2. Observations

We report H_2CO observations performed at the Arecibo Radio Observatory[2] and the Green Bank Telescope[3] that will be described in more detail in (Ginsburg et al. 2011), with additional data to be published in a future work. Arecibo and the GBT have FWHM$\approx 50''$ beams at the observed frequencies of 4.829 and 14.488 GHz, respectively. Observations were carried out in a position-switched mode with 3 and 5.5′ offsets for the Arecibo and GBT observations respectively.

The Boston University / Five-College Radio Astronomy Observatory Galactic Ring Survey ^{13}CO data was also used. The BU FCRAO GRS (Jackson et al. 2006) is a survey of the Galactic plane in the ^{13}CO 1-0 line with $\sim 46''$ resolution. We used reduced data cubes of the $\ell = 43$ region.

2.1. A non-star-forming molecular cloud

We examine the line of sight towards G43.17+0.01, also known as W49. In a large survey, we observed two lines of sight towards W49, the second at G43.16-0.03. Both are very bright continuum sources, and two GMCs are easily detected in both H_2CO absorption and ^{13}CO emission. Figure 1 shows the spectra levels dominated by W49 itself, but with clear foreground absorption components. The continuum level subtracted from the spectra are 73 K at 6 cm and 11 K at 2 cm for the south component, and 194 K at 6 cm and 28 K at 2 cm for the north component.

We focus on the "foreground" line at ~ 40 km s^{-1}, since it is not associated with the extremely massive W49 region. The cloud, known as GRSMC 43.30-0.33 (Simon et al. 2001), was confirmed to have no associated star formation in that work. Additional H_2CO spectra of surrounding sources that are bright at 8-1100 μm and within the ^{13}CO contours of the cloud show that they are all at the velocity of W49 and therefore are not associated with these foreground clouds.

The H_2CO lines are is observed in the outskirts of the cloud, not at the peak of the ^{13}CO emission. The cloud spans $\sim 0.6°$, or ~ 30 pc at $D = 2.8$ kpc (Roman-Duval et al. 2009). It is detected in $1_{10} - 1_{11}$ absorption at all 6 locations observed in H_2CO (Figure 2), but $2_{11} - 2_{12}$ is only detected in front of the W49 HII region because of the higher sig(long dash, i.e., --)location. The detected ^{13}CO and H_2CO lines are fairly narrow, with H_2CO FWHM $\sim$ 1.3-2.8 km s^{-1} and ^{13}CO widths from 1.8-5.9 km s^{-1}. The ^{13}CO lines are 50% wider than the H_2CO lines.

The highest ^{13}CO contours are observed as a modest infrared dark cloud in Spitzer 8 μm images, but no dust emission peaks are observed at 500 μm or 1.1 m--- associated with the dark gas. This is an indication that any star formation, if present, is weak - no massive dense clumps

[2]The Arecibo Observatory is part of the National Astronomy and Ionosphere Center, which is operated by Cornell University under a cooperative agreement with the National Science Foundation.

[3]The National Radio Astronomy Observatory operates the GBT and VLA and is a facility of the National Science Foundation operated under cooperative agreement by Associated Universities, Inc.

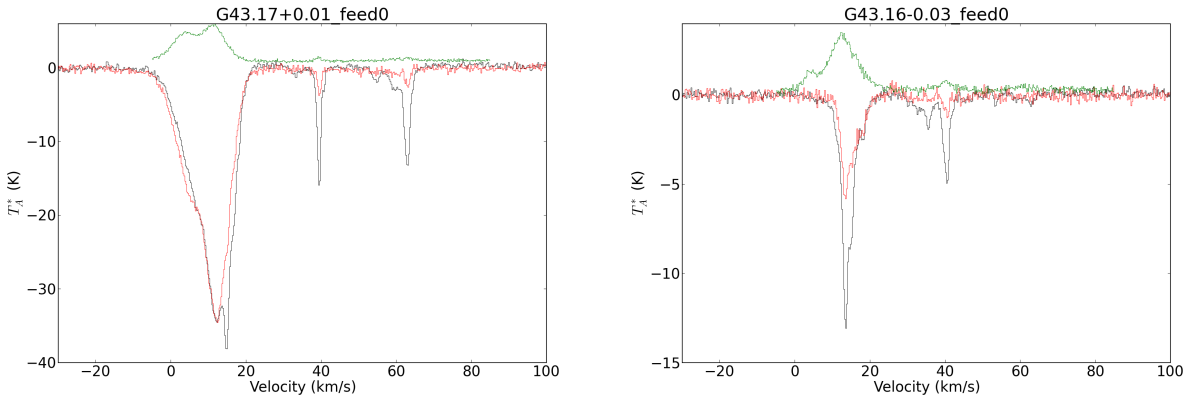

Fig. 1.— Spectra of the H_2CO $1_{10}-1_{11}$ (black), $2_{11}-2_{12}$ (red), and ^{13}CO 1-0 (green) lines towards G43.17+0.01 (left) and G43.16-0.03 (right). The H_2CO spectra are shown continuum-subtracted, and the ^{13}CO spectrum is offset by 1 K for clarity. The GBT $2_{11}-2_{12}$ spectra are multiplied by a factor of 9 so the smaller lines can be seen. CUT for letter-form

are present within this cloud.

The cloud has mass $M_{CO} = 1.5 \times 10^4\ M_\odot$ in a radius $r = 15$ pc, so its mean density is $n(H_2) \approx 15$ cm^{-3} assuming spherical symmetry. If we instead assume a cubic volume, the mean density is $n(H_2) \sim 8$ cm^{-3}. For an oblate spheroid, with minor axis 0.1× the other axes, the mean density is $n \sim 150$cm^{-3}, which we regard as a conservative upper limit. Simon et al. (2001) report a mass $M_{CO} = 6 \times 10^4 M_\odot$ and $r = 13$ pc, yielding a density $n(H_2) = 100$ cm^{-3}, which is consistent with our estimates but somewhat higher than measured by Roman-Duval et al. (2010) because of the improved optical depth corrections in the latter work.

(add space)

Why this notation here? Couldn't you write it as before: n(H_2) = 10--10^8 cm^-3?

3. Modeling H_2CO

In order to infer densities using the H_2CO densitometer, we use the low-temperature collision rates given by Troscompt et al. (2009) with RADEX (van der Tak et al. 2007) to build a grid of predicted line properties covering densities from $10 - 10^8$ H_2 cm^{-3}, temperatures from 5-50 K, column densities N(o-H_2CO) from $10^{11} - 10^{16}$ cm^{-2}, and ortho-to-para ratios from $10^{-3} - 3$.

The H_2CO densitometer measurements are shown in Figure 3. The figures show optical depth spectra, given by the equation

$$\tau = -\ln\left(\frac{S_\nu + 2.73}{\bar{C}_\nu + 2.73}\right) \quad (1)$$

where S_ν is the spectrum (with continuum included) and $\bar{C}_\nu$ is the measured continuum, both in Kelvins. The cosmic microwave background temperature is added to the continuum since H_2CO can be seen in absorption against it, though towards W49 it is negligible.

Maybe add units of Kelvin here explicitely, because you say in the text that S_nu and C_nu are in Kelvin, too.

Somewhat confusing notation. Can you clarify which part is the name and what the 40 km/s mean?

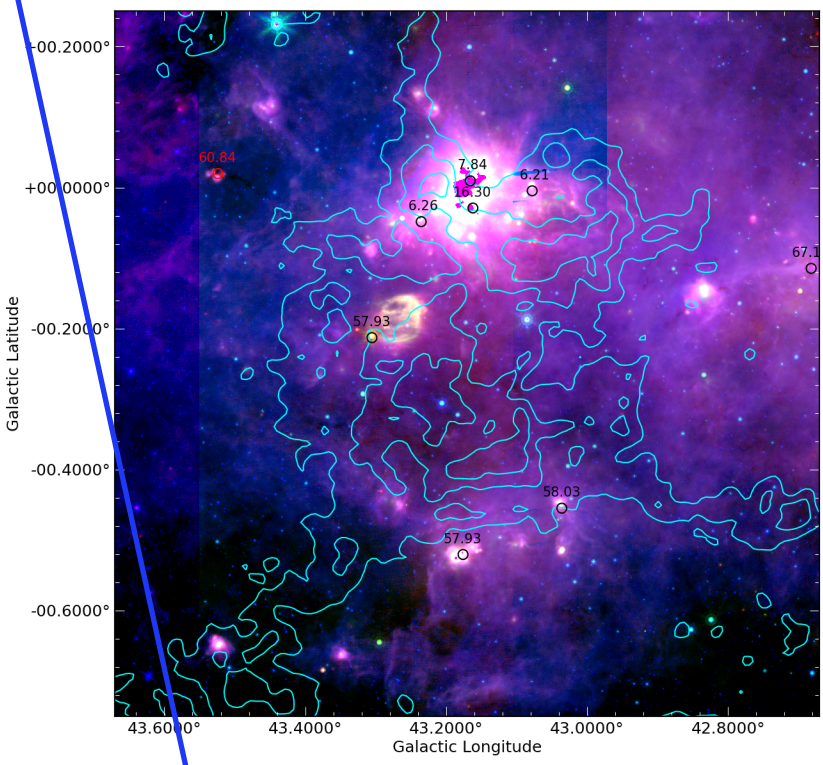

Fig. 2.— The G43 40 km s^{-1} cloud. The background image shows Herschel SPIRE 70 μm (red), Spitzer MIPS 24 μm (green), and Spitzer IRAC 8 μm (blue) in the background with the ^{13}CO integrated image from $v = 36$km s^{-1} to $v = 43$km s^{-1} at contour levels of 1, 2, and 3 K superposed in orange contours. The red and black circles show the locations of H_2CO pointings, and their labels indicate the LSR velocity of the strongest line in the spectrum. The W49 HII region is seen behind some of the faintest ^{13}CO emission that is readily associated with this cloud. The dark swath in the 8 and 24 μm emission going through the peak of the ^{13}CO emission in the lower half of the image is likely a low optical depth infrared dark cloud associated with this GMC.

Where are the orange contours?

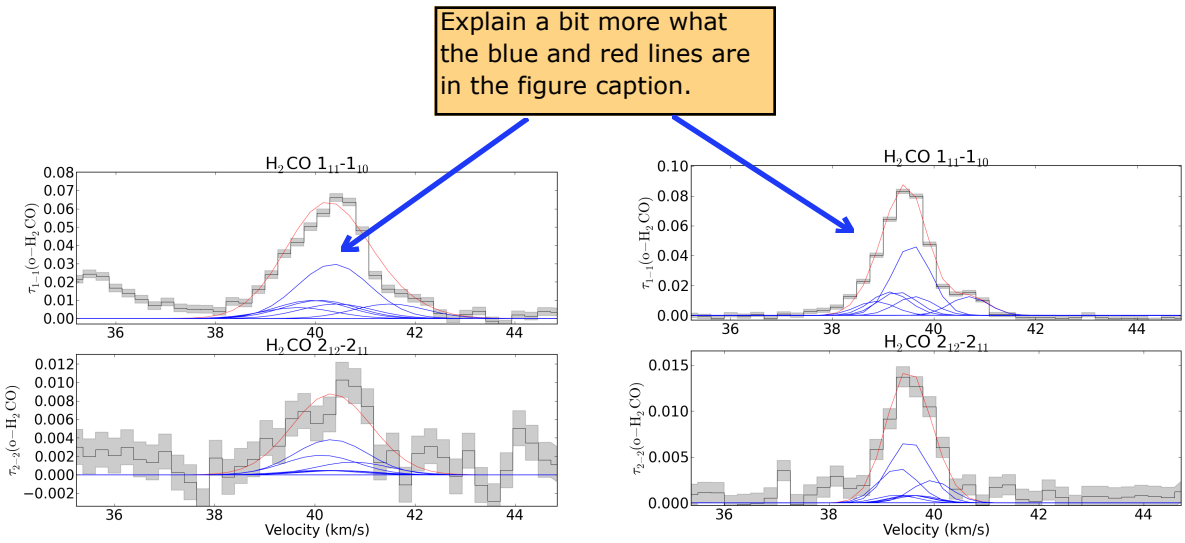

Fig. 3.— Optical depth spectra of the $1_{10} - 1_{11}$ and $2_{11} - 2_{12}$ lines towards the two W49 lines of sight, G43.16 (left) and G43.17 (right). The fitted parameters, along with the statistical 1-σ errors, are shown in the legend. [CUT] The optical depth ratio falls in a regime where temperature has very little effect and there is no degeneracy between low and high densities.

We performed line fits to both lines simultaneously using a Markov-chain monte-carlo approach, assuming uniform priors across the modeled parameter space and independent gaussian errors on each spectral bin. The density measurements are very precise, with $n \approx 23,000^{+9300}_{-7700}$ cm^{-3} (95% confidence interval) and $n \approx 20,400^{+12000}_{-10000}$ cm^{-3} for G43.17+0.01 and G43.16-0.03 respectively. While this is a precise measurement of gas density, we now need to examine exactly what gas we have measured the density of.

Since the W49 line of sight is clearly on the outskirts of the cloud, not through its center, such a high density is unlikely to be an indication that this line of sight corresponds to a centrally condensed density peak (e.g., a core). The comparable density observed through two different lines of sight separated by ~ 2 pc also supports this idea.

4. Turbulence and H_2CO

Supersonic interstellar turbulence can [gas density] zed by its driving mode, Mach number $\mathcal{M}$, and magnetic field strength. Assuming the ~~distribution~~ follows a lognormal distribution, defined as

$$P_V(s) = \frac{1}{\sqrt{2\pi\sigma_s^2}} \exp\left[-\frac{(s+\sigma_s^2/2)^2}{2\sigma_s^2}\right] \quad (2)$$

where the subscript V indicates that this is a volumetric density distribution function. The width of the turbulent density distribution is given by

$$\sigma_s^2 = \ln\left(1 + b^2\mathcal{M}^2\frac{\beta}{\beta+1}\right) \quad (3)$$

...with s = ln(rho/rho_0) and...

(Padoan & Nordlund 2011; Molina et al. 2012)

I would rather call it "density contrast", because it can also be negative in which case it's an underdensity rather than a overdensity. Actually, move that further up when s appears the first time.

where $\beta = 2c_s^2/v_A^2 = 2\mathcal{M}_A^2/\mathcal{M}^2$ and b ranges from 1/3 (solenoidal, divergence-free forcing) to 1 (compressive, curl-free) forcing (Federrath et al. 2010). The parameter s is the logarithmic overdensity, $s \equiv \ln(\rho/\rho_0)$.

b~

b~

The observed H_2CO ratio roughly depends on the *mass-weighted* probability distribution function (as opposed to the volume-weighted distribution function, which is typically reported in simulations). We first examine the implications assuming a lognormal distribution for the mass-weighted density.

Say what that is: I guess it's Large Velocity Gradient, but should be spelled out once.

We use LVG models of the H_2CO lines, which are computed assuming a fixed local density, as a starting point to model the observations of H_2CO in turbulence. Starting with a fixed *volume-averaged* density ρ_0, we compute the observed H_2CO optical depth in both the $1_{10}-1_{11}$ and $2_{11}-2_{12}$ line by averaging over the mass-weighted density distribution.

m versus M; v versus V. Use consistent notation. Define P_M = rho*P_V (see Li, Klessen, Mac Low 2003) and Federrath & Klessen (2013).

Add a short sentence on how good/bad that approximation is.

$$\tau(\rho_0) = \int_{-\infty}^{\infty} \frac{\tau_p(\rho)}{N_p} P_m(\ln \rho/\rho_0) d\ln\rho$$

$\tau_p(\rho)/N_p$ is the optical depth *per particle* at a given density, where N_p is the column density (per km s^{-1} pc^{-1}) from the LVG model. We assume a fixed abundance of o-H_2CO relative to H_2 (i.e., the H_2CO perfectly traces the H_2). Figure 4 shows the result of this integral for an abundance of o-H_2CO relative to H_2 $X(\text{o-}H_2CO) = 10^{-9}$, where the x-axis shows $\rho_0 = n(H_2)$ and the Y-axis shows the observable optical depth ratio of the two H_2CO centimeter lines.

Rather use s and ds instead of ln(rho) and d ln(rho).

comma? Maybe rephrase to avoid having H2 and X directly together. Might be confused with H2 times X.

4.1. Turbulence and GRSMC 43.30-0.33

We use the density measurements in GSRMC 43.30-0.33 to infer properties of that cloud's density distribution.

We measure the abundances of o-H_2CO relative to ^{13}CO, $X(\text{o-}H_2CO/^{13}CO) = 3.2\times10^{-4}$ and 9.8×10^{-4} for G43.16 and G43.17 respectively, or relative to H_2, 5.8×10^{-10} and 1.7×10^{-9}, which are entirely consistent with other measurements of $X_{\text{o-}H_2CO}$ and allow us to use Figure 4 for this analysis. The observed formaldehyde line ratio $\tau_{1-1}/\tau_{2-2} \sim 6$, while the volume averaged mean density of the cloud $8 \lesssim \rho_0 < 150$.

Can you quote a few studies?

units?

What do you mean by 'allowed values'. I think it would be good to elaborate on this and explain the analysis (computation) of b, by giving the reader more of the intermediate steps that lead to your measurement from figure 4.

a temperature $T = 10$ K, consistent with both the H_2CO and CO observations 2004), the sound speed in molecular gas is $c_s = 0.19$ km s^{-1}. The observed line 3.17 is 0.95 km s^{-1} for H_2CO and 1.7 km s^{-1} for ^{13}CO 1-0, so the Mach number of is $\mathcal{M} \approx 5.1 - 9.1$.

(3)

me the density distribu is lognormal, we can determine the values of the 'com-efficient' b from Equation 3. Assuming the thermal dominates the magnetic pressure ($\beta >> 1$), the allowed values of σ_s given the line-width based limits on $\mathcal{M}$ range from 1.8-2.1 for $b = 1$ and 1.2-1.5 for $b = 1/3$. If magnetic pressure is significant, the allowed values of σ_s drop.

Is this the 1D Mach number(i.e., only along the line of sight), or the 3D Mach number, which (if isotropy is assumed) would be Mach_3D ~ sqrt(3) * Mach_1D? I'm asking, because in the theory equations (e.g., equation 3), the 3D Mach number is used. We just have to keep this in mind when computing things like b. Of course, the same argument applies to sigma_s, which is actually the 3D log-density dispersion. I'm just asking whether you have taken those considerations into account?

Maybe rephrase to introduce Figure 4 and then explain Figure 4 in detail. That's missing here. Currently, you basically jump to the measurement of b very quickly.

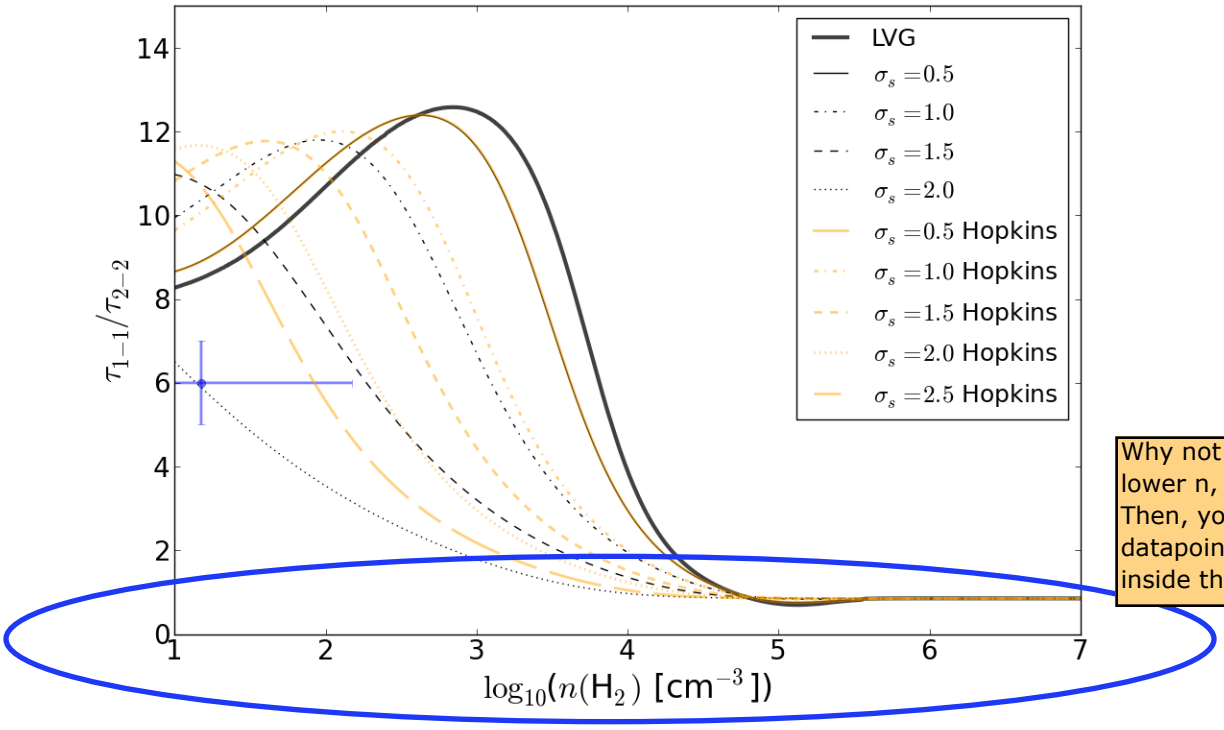

Why not extend the range to lower n, e.g., log(n) = -1? Then, your measured datapoint would also be fully inside the plot window.

Fig. 4.— The predicted H_2CO $1_{10} - 1_{11}/2_{11} - 2_{12}$ ratio as a function of volume-weighted mean density for a fixed abundance relative to H_2 $X(\text{o-}H_2CO) = 10^{-9}$ and H_2 ortho/para ratio 1.0. The legend shows the effect of smoothing with different lognormal mass distributions as described in Equation 3. The solid line, labeled LVG, shows the predicted ratio with no smoothing (i.e., a δ-function density distribution). The blue errorbars show the G43.17 H_2CO measurement and the GSRMC 43.30-0.33 mean density.

Why 20T? Can you provide more information / intermediate steps of your analysis and comparison with data presented in Hopkins (2013)? That's needed here to understand what you did exactly.

...for the intermittency parameter T=...

Where does this actually come from?

Given that the observed mean cloud density is $n(\mathrm{H}_2) \lesssim 10^2 \mathrm{cm}^{-3}$, Figure 4 shows that only the most extreme values of σ_s can explain the mean density. Even if the cloud is extremely oblate, e.g. with a line-of-sight axis 0.1× the plane-of-sky axes, $\sigma_s > 1.5$ is required.

In order to achieve a self-consistent mass and volume PDF, we use the Hopkins (2013) distribution with the fitted relation $T = 0.25 \ln(1 + 0.25\sigma_s^4(1+T)^{-6}$. Using the $\sigma_s = 2.5$ distribution, which is just consistent with the observations, $T = 0.29$, and based on Hopkins (2013) Figure 3, the compressive Mach number $\mathcal{M}_c$ $20T \approx 5.8$. Compared to the mach number restrictions from the line width, this $\mathcal{M}_C$ implies a compressive-to-total ratio $b > 0.6$.

The restrictions on σ_s using either assumed density [illegible] are strong indications that compressive forcing must be a significant, if not dominant, mode in this molecular cloud. All of the systematic uncertainties tend to require a *greater* b value. Temperatures in GMCs are typically 10-20 K: warmer temperatures increase the sound speed, decrease the Mach number, and therefore decrease σ_s. Stronger (i.e. non-negligible) magnetic fields decrease σ_s.

no comma?

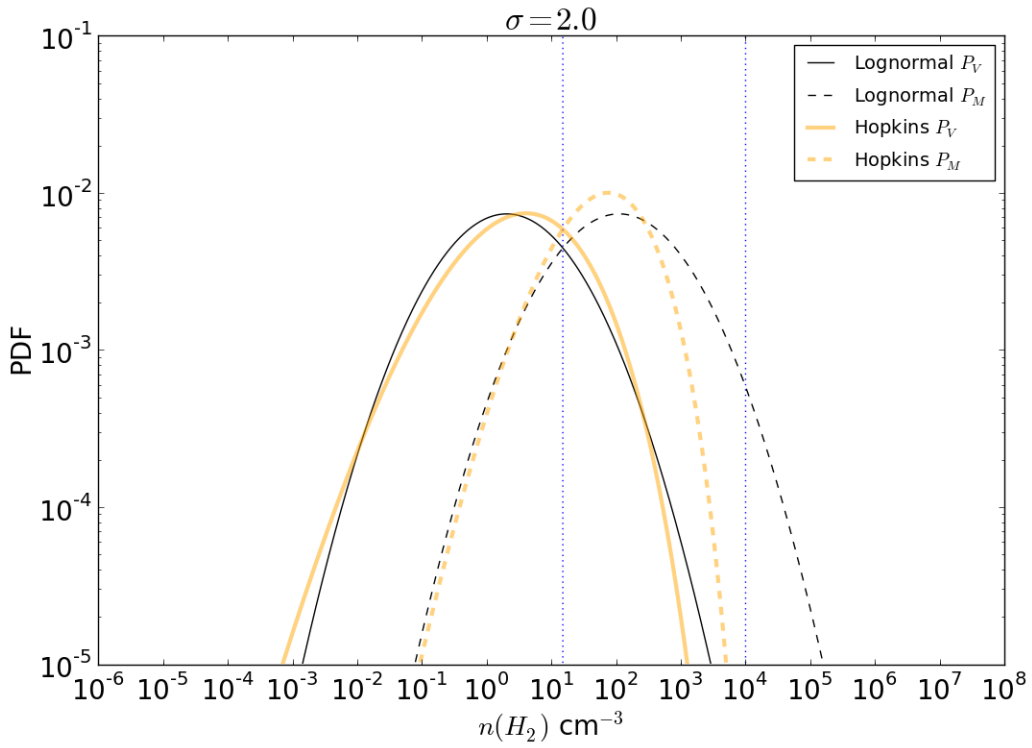

Fig. 5.— Example volume- and mass-weighted density distributions with $\sigma_s = 2.0$. The vertical dashed lines show $\rho = 15$ and $\rho = 10^4$, approximately corresponding to the volume-averaged mean density of GRSMC 43.30 and the $\mathrm{H_2CO}$-derived density

Needs to be discussed in the text.

5. Conclusions

We demonstrate the use of a novel method of inferring the shape of the density probability distribution in a molecular cloud using H_2CO densitometry in conjunction with ^{13}CO-based estimates of total cloud mass.

Our data show evidence for compressively driven turbulence in a non-star-forming giant molecular cloud. Such high compression in a fairly typical GMC indicates that compressive driving is probably a common feature of all molecular clouds.

Facilities: GBT, Arecibo, VLA, FCRAO, CSO

REFERENCES

Chabrier, G. & Hennebelle, P. 2010, ApJ, 725, L79

Darling, J. & Zeiger, B. 2012, ApJ, 749, L33

Federrath, C., Chabrier, G., Schober, J., Banerjee, R., Klessen, R. S., & Schleicher, D. R. G. 2011, Physical Review Letters, 107, 114504

Federrath, C. & Klessen, R. S. 2013, ApJ, 763, 51

Federrath, C., Klessen, R. S., & Schmidt, W. 2008, ApJ, 688, L79

—. 2009, ApJ, 692, 364

Federrath, C., Roman-Duval, J., Klessen, R. S., Schmidt, W., & Mac Low, M.-M. 2010, A&A, 512, A81

Ginsburg, A., Darling, J., Battersby, C., Zeiger, B., & Bally, J. 2011, ApJ, 736, 149

Hennebelle, P. & Chabrier, G. 2011, ApJ, 743, L29

—. 2013

Hopkins, P. F. 2012, MNRAS, 423, 2037

Hopkins, P. F. 2013, Monthly Notices of the Royal Astronomical Society, 430, 1653

Jackson, J. M. et al. 2006, ApJS, 163, 145

Kainulainen, J., Federrath, C., & Henning, T. 2013

Kainulainen, J. & Tan, J. C. 2012, ArXiv e-prints

Konstandin, L., Girichidis, P., Federrath, C., & Klessen, R. S. 2012, ApJ, 761, 149

Kritsuk, A. G., Norman, M. L., & Wagner, R. 2011, ApJ, 727, L20

Krumholz, M. R., McKee, C. F., & Klein, R. I. 2005, Nature, 438, 332

Mangum, J. G. & Wootten, A. 1993, ApJS, 89, 123

Molina, F. Z., Glover, S. C. O., Federrath, C., & Klessen, R. S. 2012, MNRAS, 423, 2680

Padoan, P., Haugbølle, T., & Nordlund, Å. 2012, ApJ, 759, L27

Padoan, P. & Nordlund, Å. 2011, ApJ, 730, 40

Padoan, P., Nordlund, Å., Kritsuk, A. G., Norman, M. L., & Li, P. S. 2007, ApJ, 661, 972

Plume, R. et al. 2004, ApJ, 605, 247

Roman-Duval, J., Jackson, J. M., Heyer, M., Johnson, A., Rathborne, J., Shah, R., & Simon, R. 2009, ApJ, 699, 1153

Roman-Duval, J., Jackson, J. M., Heyer, M., Rathborne, J., & Simon, R. 2010, ApJ, 723, 492

Simon, R., Jackson, J. M., Clemens, D. P., Bania, T. M., & Heyer, M. H. 2001, ApJ, 551, 747

Tang, X. D., Esimbek, J., Zhou, J. J., Wu, G., Ji, W. G., & Okoh, D. 2013, A&A, 551, A28

Troscompt, N., Faure, A., Wiesenfeld, L., Ceccarelli, C., & Valiron, P. 2009, A&A, 493, 687

van der Tak, F. F. S., Black, J. H., Schöier, F. L., Jansen, D. J., & van Dishoeck, E. F. 2007, A&A, 468, 627

Wiesenfeld, L. & Faure, A. 2013, ArXiv e-prints